

## Article

# Molecular Docking, Tyrosinase, Collagenase, and Elastase Inhibition Activities of Argan By-Products

Hicham Mechqoq <sup>1</sup>, Sohaib Hourfane <sup>2</sup>, Mohamed El Yaagoubi <sup>1</sup>, Abdallah El Hamdaoui <sup>1</sup>, Jackson Roberto Guedes da Silva Almeida <sup>3</sup>, Joao Miguel Rocha <sup>4,5</sup> and Nouredine El Aouad <sup>2,\*</sup>

- <sup>1</sup> Laboratory of Biotechnologies and Valorization of Natural Resources, Faculty of Sciences, University Ibn Zohr-Agadir, Agadir 80000, Morocco; h.mechqoq@gmail.com (H.M.); elyaagoubi08@gmail.com (M.E.Y.); hmd\_abdl@hotmail.com (A.E.H.)
- <sup>2</sup> Research Team on Biological Engineering, Agrifood and Aquaculture, Polydisciplinary Faculty of Larache, Abdelmalek Essaadi University, Tetouan 95000, Morocco; hourfane.sohaib@gmail.com
- <sup>3</sup> Center for Studies and Research of Medicinal Plants (NEPLAME), Federal University of Vale do São Francisco, Petrolina 56304-205, Brazil; jackson.guedes@univasf.edu.br
- <sup>4</sup> LEPABE—Laboratory for Process Engineering, Environment, Biotechnology and Energy, Faculty of Engineering, University of Porto, Rua Dr. Roberto Frias, 4200-465 Porto, Portugal; jmfrocha@fe.up.pt
- <sup>5</sup> ALiCE—Associate Laboratory in Chemical Engineering, Faculty of Engineering, University of Porto, Rua Dr. Roberto Frias, 4200-465 Porto, Portugal
- \* Correspondence: n.elaouad@uae.ac.ma; Tel.: +212-661-186-156

**Abstract:** The argan tree (*Argania spinosa* (L.) Skeels) is one of the most important floristic resources in Morocco. This Moroccan endemic tree is known for its numerous therapeutic and medicinal uses. In addition to some medicinal and cosmetic uses, argan fruit pulp and press cake are traditionally used by the Berber population for heating and feeding livestock. Molecular docking is an in silico approach that predicts the interaction between a ligand and a protein. This approach is mainly used in chemistry and pharmacology of natural products as a prediction tool with the purpose of selecting plant extracts or fractions for in vitro tests. The aim of this research is to study the evaluation of potential tyrosinase, collagenase, and elastase inhibitory activities of argan fruit press-cake and pulp extracts. Extracts were evaluated for their total phenolic content (TPC), and the major polyphenols of both press-cake and pulp extracts were submitted to molecular docking in order to determine the mechanisms of action of these compounds. Obtained results revealed that fruit pulp had the strongest dermocosmetic activities, as well as the highest TPC, with values above 55 mg gallic acid equivalent per gram of dry matter ( $\text{mg}_{\text{eq AG}}/\text{g}_{\text{DM}}$ ). Moreover, those results were positively correlated with the docking findings, suggesting that the pulp lead compounds have higher affinity with tyrosinase, collagenase, and elastase action sites. The results here presented are very promising and open new perspectives for the exploitation of argan-tree by-products as cosmetic agents towards the development of new anti-aging products.

**Keywords:** argan tree by-products; press cake; fruit pulp; natural dermocosmetics; molecular docking; inhibition; tyrosinase; collagenase; elastase



**Citation:** Mechqoq, H.; Hourfane, S.; El Yaagoubi, M.; El Hamdaoui, A.; da Silva Almeida, J.R.G.; Rocha, J.M.; El Aouad, N. Molecular Docking, Tyrosinase, Collagenase, and Elastase Inhibition Activities of Argan By-Products. *Cosmetics* **2022**, *9*, 24. <https://doi.org/10.3390/cosmetics9010024>

Academic Editor: Enzo Berardesca

Received: 28 January 2022

Accepted: 11 February 2022

Published: 14 February 2022

**Publisher's Note:** MDPI stays neutral with regard to jurisdictional claims in published maps and institutional affiliations.



**Copyright:** © 2022 by the authors. Licensee MDPI, Basel, Switzerland. This article is an open access article distributed under the terms and conditions of the Creative Commons Attribution (CC BY) license (<https://creativecommons.org/licenses/by/4.0/>).

## 1. Introduction

Skin is a layer of soft and flexible tissue covering the bodies of vertebrates and humans. This layer is considered an organ, and it is known for its protection, regulation, and sensation functions [1]. Human skin is mainly composed of three primary layers (epidermis, dermis, and hypodermis). The epidermis is composed of a nonviable layer called the stratum corneum, which acts as a barrier for the body, protecting it from external agents and maintaining cutaneous hydration [2], whereas the dermis is essentially composed of connective tissue (collagen and elastin), sweat glands, and nerves. Its main role is the support of the epidermis. Collagen fibers give the skin strength, while elastin fibers

are responsible for skin elasticity and resistance [3]. Hair is one of the defining external characteristics of humans. It is a protein filament that grows from dermis follicles, and grows everywhere except on glabrous skin such as the palms of the hands and soles of the feet [4]. Hair's main functions are to protect the skin from physical damage and sunlight, improve thermal regulation, and increase skin surface sensitivity to stimuli [5]. Aging is a degenerative process that consists of the accumulation of physiological changes over time. There are two types of aging: intrinsic aging induced by inherited genetic factors, and extrinsic aging caused by environmental factors such as sun exposure, nutrition, and pollution [6]. The aging process involves the skin and other communicating systems, including the bone, cartilage, and hair [7]. The production of reactive oxygen species (ROS) through ultraviolet (UV) radiations is thought to contribute to or enhance the process of skin aging [8]. Concerning the hair, the main aging process can be monitored on hair growth and hair color [4].

The argan tree (Figure 1) is an endemic plant that grows in the southwestern areas of Morocco, and is known for its oil extracted from fruit kernels. This oil is widely used for nutrition by the Berber communities of Morocco and is recognized for its nutritional and dermatologic properties. Despite being mostly used for nutrition, argan oil is particularly recommended for treatment of dermatosis and for skin care. In fact, this oil has been proven to have good skin-hydration potential due to its chemical composition [9].



**Figure 1.** General aspect of the argan tree (*Argania spinosa* (L.) skeels).

During the argan-oil extraction process, two by-products are generated: fruit pulp and press cake. These by-products are used by the Moroccan Berber population for tanning skins, cattle grazing, and skin care. The pulp and cake's biological properties have been reported in many ethnobotanical surveys. In contrast with argan fruit shells, they are also easier to study due to their friable structure, which greatly facilitates the extraction of secondary metabolites. Moreover, several studies have suggested the presence of very interesting dermocosmetic properties [10–12].

The present research effort aims at extracting secondary metabolites from argan press cakes and fruit pulp, and further evaluating their potential dermocosmetic activities, *viz.* anti-tyrosinase, anti-collagenase, and anti-elastase. The main compounds of argan extracts were selected from literature and submitted to molecular docking in order to identify their mechanisms of action. To the best of our knowledge, this paper is the first report of the dermocosmetic activities of argan by-products.

## 2. Materials and Methods

### 2.1. Chemicals and Reagents

Cyclohexane, dichloromethane, methanol, ethanol, sodium carbonate ( $\text{Na}_2\text{CO}_3$ ), Folin–Ciocalteu reagent, and gallic acid were obtained from Alfa Aesar GmbH & Co. (Karlsruhe, Germany). For tyrosinase inhibition assay, mushroom tyrosinase (lyophilized powder  $\geq 1000$  units/mg; EC Number 1.14.18.1), 3,4-dihydroxy-L-phenylalanine (L-DOPA), dimethylsulfoxide (DMSO), phosphate-buffered saline (PBS), and kojic acid were purchased from Sigma-Aldrich (Paris, France). For collagenase inhibition assay, collagenase from *Clostridium histolyticum* ( $\geq 1$  FALGPA units/mg; EC number: 232-582-9), fluorogenic substrate peptide MMP-2 (*MCA-Pro-Leu-Ala-Nva-DNP-Dap-Ala-Arg-NH2*), and chlorhexidine were acquired from Sigma-Aldrich. Finally, porcine pancreatic elastase type IV ( $\geq 4$  units/mg protein; EC Number 254-453-6), *N-succinyl-Ala-Ala-Ala-p-nitroanilide* (EC Number 257-823-5), tris(hydroxymethyl)aminomethane hydrochloride (Trizma-HCl), and elastinal were purchased from Sigma-Aldrich.

### 2.2. Plant Material

Argan fruits were collected in Ait Baha (Chtouka-Ait Baha, Morocco) in the summer of 2019. After harvest, fruit was dried and pulped. Resulting nuts were manually broken to separate argan shell from kernels (Figure 2). Approximately one half of the kernels were roasted for 30 min at 110 °C using a mechanical roaster controlled using a Testo 945 sensor/thermometer (Testo, Casablanca, Morocco). Roasted and unroasted kernels were mechanically pressed using Komet DD 85 G presses (IBG Monforts Oekotec GmbH, Mönchengladbach, Germany). Argan press cakes (unroasted and roasted) and fruit pulp were recovered from the cooperative, hermetically sealed in amber bags, and stored at 4 °C until further use.



**Figure 2.** Manual extraction of kernel from the argan shells (a), fruit shells (b), and kernels (c).

### 2.3. Extraction Methods

#### 2.3.1. Supercritical Fluid Extraction

Supercritical fluid extractions (SFE) were carried out exclusively on the unroasted and roasted press cakes using an SFE 1–2 pilot-scale apparatus (SEPALEX, Champigneulle, France), composed of a  $\text{CO}_2$  tank, a  $\text{CO}_2$  pump (that can deliver up to 10 kg/h), extraction vessels with volumes of 1 and 2 L, separators, a co-solvent pump, and a cooling system with glycol. All the extractions were carried out at 45 °C in order to avoid the deterioration of thermosensitive compounds. Briefly, the argan cake was reduced to powder and put in a 1 L stainless-steel extraction basket; the latter was placed in the extractor prior to the extractions. For each press-cake sample, three successive extractions were carried out: the first solely with  $\text{CO}_2$  (10 MPa), the second with  $\text{CO}_2$  and 1% ethanol (25 MPa), and the last with  $\text{CO}_2$  and 5% ethanol (25 MPa). Each extraction was carried out in triplicate (3 replicates of sample extraction). Samples containing solvent were further evaporated using a rotary evaporator (BUCHI R-100), lyophilized (CHRIST alpha 1–2, Osterode, Germany), and stored in amber vials at  $-4$  °C.

### 2.3.2. Ultrasound-Assisted Extraction

Ultrasound-assisted extractions (UAE) were performed on the argan press cakes (unroasted and roasted) and fruit pulp using a P300H ultrasonic bath (Elma Schmidbauer, Singen, Germany). To achieve this, 300 g of argan press cakes and pulp were placed separately in Erlenmeyers and extracted consecutively with 1500 mL of cyclohexane (Chex), dichloromethane (DCM), methanol (MeOH), and deionized water (H<sub>2</sub>O). A 30 min period of ultrasound-assisted extraction was used for each extraction solvent. All experiment extractions were performed in triplicate (3 replicates of sample extraction), and the extracts were further evaporated to dryness, lyophilized, and stored in amber bottles at −4 °C.

### 2.3.3. Determination of the Extraction Yields

The extraction yields of the argan by-product extracts obtained by SFE and UAE were calculated using the Equation (1) below:

$$\text{Yield of Extraction (\%)} = \frac{\text{Extract weight (g)}}{\text{Plant material (press-cake or pulp) weight (g)}} \times 100 \quad (1)$$

## 2.4. Dermocosmetic Activities

### 2.4.1. Tyrosinase Inhibition Activity

The ability of natural products and plant extracts to inhibit the oxidation of L-DOPA (L-3,4-dihydroxyphenylalanine) [13], to dopaquinone and subsequently to dopachrome by the tyrosinase enzyme was investigated, employing a protocol from Masuda et al. (2008) [14] with slight modifications. Prior to the assay, the samples were dissolved in dimethyl sulfoxide (DMSO) (10 mg/mL) and diluted in proper concentration of phosphate buffer (PBS). The final concentrations of DMSO in samples never exceeded 2%. In a microplate of 96 wells (VWR, Greiner, Spain), 40 µL of samples, 80 µL of 1/15 M phosphate buffer, and 40 µL of mushroom tyrosinase (92 units/mL) were mixed. The microplate was incubated for 10 min at 25 °C, then 40 µL of L-DOPA (2.5 mM) were added. After incubation, the absorbance was measured at a wavelength of 475 nm using a M200 Pro plate reader (TECAN, Männedorf, Switzerland). Kojic acid was used as positive control. The percentage inhibition of the tyrosinase activity was calculated by the following Equation (2):

$$\text{Tyrosinase inhibition (\%)} = \frac{(A - B) - (C - D)}{(A - B)} \times 100 \quad (2)$$

where A is the control [without (w/o) sample], B is the blank (w/o sample, w/o tyrosinase), C is the sample, and D is the blank sample (w/o tyrosinase).

Extracts were initially tested at 200 µg/mL. Samples that inhibited dopachrome production—and therefore the enzyme activity over 70% at this concentration, when compared to the reference control—were considered the most promising and were further tested at lower concentrations (consecutively at 150 and 75 µg/mL), in order to calculate the half-maximal inhibitory concentration (IC<sub>50</sub>) values.

### 2.4.2. Collagenase Inhibition Activity

The collagenase inhibitory potential was determined using the spectrofluorimetric method previously described by Michailidis et al. (2019) [15] with slight modifications. In this experimental assay, a fluorogenic substrate (metalloproteinase-2) was degraded by collagenase, producing fluorescent signal. For this assay, collagenase from *Clostridium histolyticum* (EC number: 232-582-9; Sigma-Aldrich) was prepared in Trizma-base buffer (10 mM, pH = 7.3). In a 96-well microplate, 120 µL of buffer, 40 µL of sample, and 40 µL of collagenase enzyme solution (60 µg/mL) were incubated at 37 °C for 10 min. Then, 40 µL of the fluorogenic substrate was added and the mixture incubated at 37 °C for 30 min. The fluorescent intensity was measured at excitation and emission wavelengths of 320 and 405 nm, respectively, using an Infinite 200 PRO series (Tecan, Männedorf, Switzerland) plate reader. The samples were evaluated at 250 µg/mL, and the extracts that

exhibited an inhibition percentage above 70% were then evaluated for lower concentrations in order to calculate the IC<sub>50</sub> values. Chlorhexidine was used as a positive control of the assay (IC<sub>50</sub> = 50 μM) [16]. Experiments were performed in three analytical replicates. The inhibition percentage of collagenase was calculated by the Formula (3):

$$\text{Collagenase inhibition (\%)} = \frac{(A - B) - (C - D)}{(A - B)} \times 100 \quad (3)$$

where A is the Control [without (w/o) sample], B is the Blank (w/o sample, w/o collagenase), C is the Sample, and D is the Blank Sample (w/o collagenase).

Extracts were initially tested at 200 μg/mL. Samples that showed enzyme inhibition activities over 80% at this concentration, when compared to the control reference (chlorhexidin), were considered the most promising and were further tested at lower concentrations (subsequently at 150 and 75 μg/mL), in order to calculate the half-maximal inhibitory concentration (IC<sub>50</sub>) values.

#### 2.4.3. Elastase Inhibition Activity

Elastase inhibition activity was evaluated according to a method previously described by Angelis et al. (2016) [17], using *N-succinyl-Ala-Ala-Ala-p-nitroanilide* (Sigma-Aldrich, EC Number 257-823-5) as substrate. Furthermore, the substrate degradation causes the release of p-nitroaniline that can be monitored spectrophotometrically at 405 nm. Porcine pancreatic elastase type IV (≥4 units/mg protein; EC Number 254-453-6, Sigma-Aldrich) and *N-succinyl-Ala-Ala-Ala-p-nitroanilide* were dissolved in Trizma-base buffer (50 mM, pH = 7.5). Thus, 70 μL of Trizma-base buffer, 10 μL of the samples, and 5 μL of elastase (0.45 U/mL) were mixed and incubated in a 96-well microplate for 10 min in darkness. Then, 20 μL of substrate (2 mM) were added in each well and the plate was incubated for 30 min. The absorbance was measured at 405 nm with an Infinite 200 PRO (Tecan) plate reader. The samples were evaluated at 200 μg/mL. Then, the most promising ones were evaluated at lower concentrations to determinate the IC<sub>50</sub> values. Elastatinal was used as a positive control, being a strong competitive inhibitor of elastase (IC<sub>50</sub> = 0.5 μg/mL). Experiments were performed in triplicate (3 analytical replicates). The inhibition percentage of elastase was calculated by the following expression (4):

$$\text{Elastase inhibition (\%)} = \frac{(A - B) - (C - D)}{(A - B)} \times 100 \quad (4)$$

where A is the Control [without (w/o) sample], B is the Blank (w/o sample, w/o elastase), C is the Sample, and D is the Blank Sample (w/o elastase).

Extracts were initially tested at 200 μg/mL. Samples that showed enzyme inhibition activities over 80% at this concentration, when compared to the control reference (elastatinal), were considered the most promising and were further tested at lower concentrations (subsequently at 150 and 75 μg/mL), in order to calculate the half-maximal inhibitory concentration (IC<sub>50</sub>) values.

#### 2.5. Determination of Total Phenolic Content

Total polyphenol content of the most promising samples was determined according to the protocol defined by Vermerris and Nicholson (2007) [18]. For that purpose, the UAE methanolic and aqueous extracts were diluted in methanol at 1 mg/mL. Then, 100 μL of sample was mixed with 2 mL of 2% sodium carbonate solution. The reaction mixture was incubated for 5 min, then 100 μL of Folin–Ciocalteu reagent was added. The mixture was incubated in the dark for 60 min. The absorbance of the samples was measured at 700 nm wavelength with an Infinite 200 PRO (Tecan). Three analytical repetitions were made for each sample. Standard solutions were prepared with different concentrations of gallic acid, and the results were expressed in mg of gallic acid equivalent per gram of dry matter (mg<sub>eqAG</sub>/g<sub>DM</sub>).

### 2.6. Molecular Docking

Molecular docking studies were performed to investigate the binding mode between eight polyphenols reported on the argan by-products and three enzymes (*viz.* tyrosinase, collagenase, and elastase) using Autodock Vina v1.1.2 (The Scripps Research Institute, La Jolla, San Diego, CA, USA) [19]. The three-dimensional (3D) structures of the tyrosinase (PDB CID: 2Y9X) [20], collagenase (PDB CID: 1CGL) [21], and elastase (PDB CID: 1BRU) [22] were downloaded from RCSB Protein Data Bank (<http://www.rcsb.org/>, accessed on 13 November 2021). For the selected ligands, the structures were downloaded from PubChem (<http://pubchem.ncbi.nlm.nih.gov>, accessed on 13 November 2021); we chose the argan press-cake and pulp-lead compounds, namely epicatechin (PubChem CID: 72276), vanillic acid (PubChem CID: 8468), *p*-hydroxybenzoic acid (PubChem CID: 135), 4-hydroxybenzyl alcohol (PubChem CID: 125), hyperoside (PubChem CID: 5281643), isoquercetin (PubChem CID: 5280804), protocatechuic acid (PubChem CID: 72), and gallic acid (PubChem CID: 370) (Figure 3).

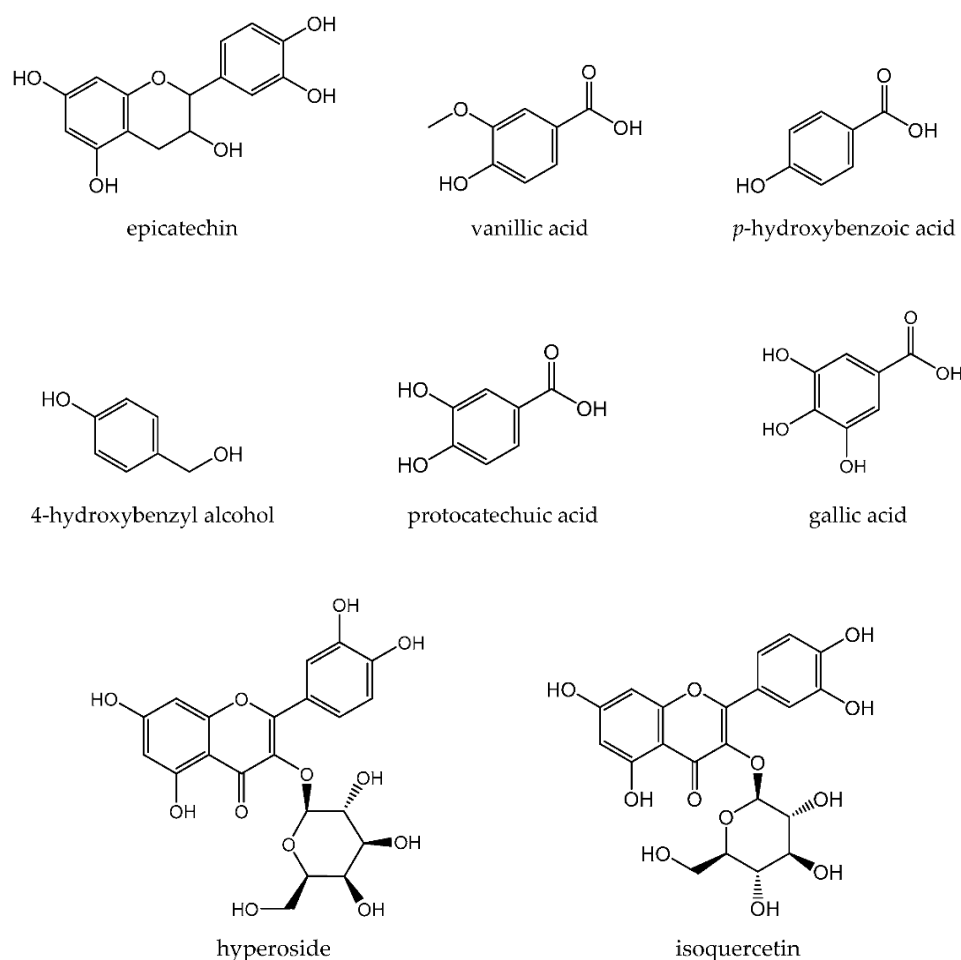


**Figure 3.** Chemical structures of the eight selected ligands.

The docking input files of both proteins and ligands were generated using AutoDockTools v1.5.6 package (ADT; Scripps Research Institute, La Jolla, San Diego, CA, USA) (Morris et al., 2009; Sanner, 1999); the proteins were prepared by removing water molecules and merging non-polar hydrogen atoms. The search grid of the key site of tyrosinase was identified as center x:  $-10.044$ , center y:  $-28.706$ , and center z:  $-43.443$ , with dimensions size x: 15, size y: 15, and size z: 15. The collagenase search grid was set as center x: 30.681, center y: 46.555, and center z:  $-0.0090$ , with dimensions size x: 60, size y: 60, and size z: 60. The elastase search grid parameters corresponded to cen-

ter x: 23.204, center y: 47.660, and center z: 17.090 with dimensions size x: 25, size y: 25, and size z: 25. Docking accuracy was increased by adjusting the exhaustiveness value to 300. After docking simulations, the best scoring pose was selected using PyMOL v1.7.6 software (DeLano Scientific LLC, Palo Alto, CA, USA) (<http://www.pymol.org/>, accessed on 13 November 2021). Then, the protein–ligand interactions were visualized using the BIOVIA Discovery Studio Visualizer v21.1.0.0 software (Accelrys, San Diego, CA, USA) (<https://discover.3ds.com/discovery-studio-visualizer-download>, accessed on 18 November 2021).

### 2.7. Statistical Analysis

All experimental data were expressed as mean  $\pm$  standard deviation by measuring three independent replicates. Means were compared statistically using the STATICA program v6.1, (Statsoft, Inc., Palo Alto, CA, USA) with Student's t test (significance level  $p < 0.05$ ).

## 3. Results and Discussion

### 3.1. Extraction Yields

After the extractions, argan press-cake and pulp extracts obtained by solvent extraction were evaporated and freeze-dried. Supercritical fluid extractions were exclusively carried out on the argan press cakes. These SFEs were undertaken to recover secondary metabolites that may have been remaining on this material. Figure 4 presents the yield values of different extracts.

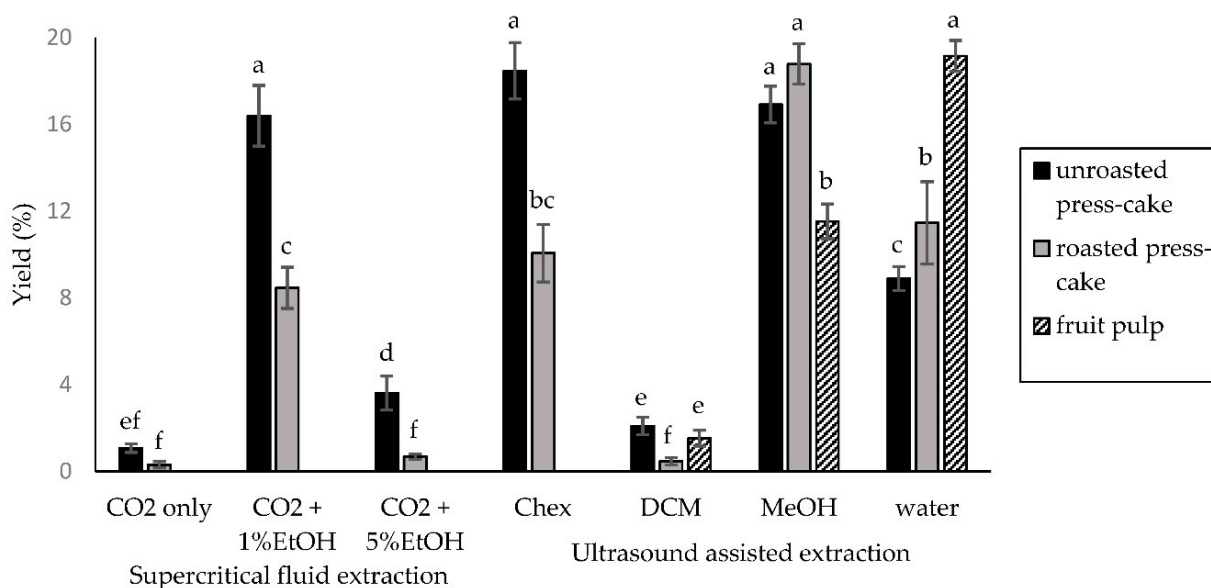


**Figure 4.** Extraction yields of argan press cakes and fruit pulp (a–f letters represent significant differences at  $p < 0.05$  by the Newman–Keuls test).

The yields of the extracts obtained with both SFE and UAE hardly exceeded 20%. The highest yield values were observed in the UAE pulp aqueous extract [(19.15  $\pm$  0.72)%], UAE roasted press-cake methanolic extract [(18.78  $\pm$  0.93)%], and UAE unroasted press-cake cyclohexane extract [(18.46  $\pm$  1.3)%], followed by the UAE unroasted press-cake methanolic extract and SFE + Ethanol 1% unroasted press-cake extract with (16.91  $\pm$  0.85)% and (16.39  $\pm$  1.4)%, respectively. Additionally, the unroasted press cake showed the highest yield values in comparison with the roasted press cake, except for the methanolic and aqueous UAE extracts. Such a phenomenon can be explained by the structural transformation of some compounds due to the Maillard reaction occurring during the kernel-roasting process [23].

Supercritical fluid extraction technology was applied in order to recover secondary metabolites from the argan press cake with a minimal environmental impact. As a matter of fact, and despite the use of ethanol as a co-solvent, this method presents the advantage of using few solvent volumes, which makes it more eco-friendly. However, this method did not achieve the expected results, giving extracts with lower yields when compared to a more conventional method such as ultrasound-assisted extraction. Taribak et al., 2013 [24] reported the use of supercritical fluid extraction on argan kernels. This technique was applied with CO<sub>2</sub> solely, and was aimed at the recovery of argan oils trapped on the kernels. The same authors showed no interest in the additional secondary metabolites that may have remained on the raw material.

Ultrasound-assisted extraction was undertaken, and a successive increasing polarity order (obtained by the means of different extraction solvents) was applied to all plant materials in order to extract all secondary metabolites. For the argan press cake, the highest yield values were obtained with cyclohexane, with a yield value higher than 18%. The presence of residual argan oil in this extract was confirmed by thin-layer chromatography (TLC). Moreover, the methanolic and aqueous extracts of the press cakes and pulp showed yield values ranging between 8 and 20%. This fraction contains more polar compounds such as polyphenols, flavonoids, coumarins, proteins, and sugars. The analysis of the bibliography showed that numerous authors who studied the argan-pulp phytochemistry were interested in its essential oils. Harhar et al. (2010) [25,26] reported essential-oil-extraction yield values between 0.06 and 0.08%. Another study published by El Monfalouti et al. (2012) [27], described the chemical analysis of argan-fruit shells, pulp, and press cake, and confirmed the presence of polyphenols on those parts; however, this study makes no mention of the extraction yields.

### 3.2. Enzyme Inhibition Assays

Tyrosinase is a multifunctional enzyme present in the melanosome membrane [28]. This enzyme catalyzes the first two steps of the melanin biosynthetic pathway in which tyrosine is converted to dopaquinone, after which the melanogenesis pathway follows two paths, the eumelanin pathway and the pheomelanin pathway [29]. This enzyme is a keystone in melanin biosynthetic metabolism [30]. The results of the tyrosinase inhibition assay of the argan press-cake and pulp extracts are summarized in Table 1.

The press-cake and pulp extracts were evaluated at a concentration of 200 µg/mL and the obtained results showed tyrosinase inhibition values lower than 60%. These values are relatively low when compared to the positive control, which showed an inhibition value of 95%. Moreover, the observation of the inhibition values disclosed that the pulp extracts were the most active, with a tyrosinase inhibition percentage of 54.74% for the methanolic extract, 23.12% for the aqueous extract, and 11.39% for the dichloromethanolic extract. This can be explained by the fact that methanolic and aqueous pulp extracts contain polyphenols, and these metabolites are good tyrosinase inhibitors. According to El Monfalouti et al., 2012 [27], the methanolic extract of fruit pulp contains polyphenols at a rate of (59.5 ± 6.3) mg/100 g of dry matter, while the press cake contains (1.97 ± 0.6) mg/100 g of dry matter. The very low phenolic content of the argan press-cake extracts may explain the results of the tyrosinase inhibition activity. In the current study, the press-cake extracts showed an inhibition percentage of less than 10% compared to the positive control (kojic acid).

In a study published by Bourhim et al. (2018) [31], the hydroalcoholic extract of argan press-cake was evaluated for its melanogenesis inhibitory activity in the genes. The authors demonstrated that the treatment of human cells with the press-cake extract allowed the reduction of tyrosinase gene expression by 47%. According to the same authors, this activity is mainly due to the saponins present in the press cake. However, these molecules are only effective on gene expression, and have no effect on the tyrosinase enzyme active sites.

**Table 1.** Percentages (mean values  $\pm$  standard deviation) of tyrosinase inhibition by argan cake and pulp extracts at 200  $\mu\text{g}/\text{mL}$ .

Extraction Method	Extraction Solvent	Plant Material	Tyrosinase Inhibition (%)	Collagenase Inhibition (%)	Elastase Inhibition (%)	
Supercritical fluid extraction(SFE)	CO <sub>2</sub> only	Unroasted press-cake	2.05 $\pm$ 1.21	1.85 $\pm$ 0.56	0 $\pm$ 0	
		Roasted press-cake	0.15 $\pm$ 0.21	2.18 $\pm$ 0.75	0 $\pm$ 0	
	CO <sub>2</sub> + 1% EtOH	Unroasted press-cake	1.03 $\pm$ 0.27	2.7 $\pm$ 0.31	1.24 $\pm$ 0.2	
		Roasted press-cake	1.23 $\pm$ 0.79	2.52 $\pm$ 0.94	1.38 $\pm$ 0.14	
	CO <sub>2</sub> + 5% EtOH	Unroasted press-cake	1.94 $\pm$ 1.01	1.32 $\pm$ 0.39	0.1 $\pm$ 0.06	
		Roasted press-cake	0.73 $\pm$ 0.19	2.4 $\pm$ 0.72	0.15 $\pm$ 0.1	
	Cyclohexane	Unroasted press-cake	0.81 $\pm$ 0.21	0.98 $\pm$ 0.13	0 $\pm$ 0	
		Roasted press-cake	1.54 $\pm$ 0.36	1.63 $\pm$ 0.51	0 $\pm$ 0	
Ultrasound-assisted extraction (UAE)	Dichloromethan	Unroasted press-cake	1.52 $\pm$ 0.38	1.54 $\pm$ 0.95	3.77 $\pm$ 1.01	
		Roasted press cake	1.11 $\pm$ 0.59	0.87 $\pm$ 0.68	3.28 $\pm$ 1.0	
	Methanol	Pulp	11.39 $\pm$ 1.23	23.6 $\pm$ 2.5	4.39 $\pm$ 2.08	
		Unroasted press cake	7.3 $\pm$ 1.63	15.09 $\pm$ 2.7	12.13 $\pm$ 1.95	
	Water	Roasted press cake	6.78 $\pm$ 1.47	19.22 $\pm$ 1.96	13.41 $\pm$ 2.1	
		Pulp	54.74 $\pm$ 3.7	52.29 $\pm$ 1.71	25.02 $\pm$ 1.69	
	Water	Unroasted press cake	5.75 $\pm$ 2.47	28.34 $\pm$ 2.62	19.63 $\pm$ 2.14	
		Roasted press cake	3.49 $\pm$ 1.04	31.43 $\pm$ 3.06	19.98 $\pm$ 1.28	
	Positive control		Pulp	23.12 $\pm$ 2.61	60.97 $\pm$ 2.36	38.41 $\pm$ 2.18
			Kojic acid	95.18 $\pm$ 2.36	<i>chlorhexidine</i>	<i>Elastrinal</i>
			98.24 $\pm$ 1.97	99.96 $\pm$ 0.02		

Over the last 20 years, a large number of phenolic compounds have been tested for their tyrosinase inhibitory potential [32–36]. So far, polyphenols are the strongest and most important tyrosinase inhibitors, and this is due to the fact that these compounds have a very high affinity with tyrosinase, especially the polyphenol glycosides [37].

As a matter of fact, these metabolites bind to the enzyme on their action sites (generally occupied by the substrate). The strength of affinity of those polyphenols can be relatively medium or high, depending on the presence or absence of additional chemical functions [38,39]. Studies have shown that some flavonoids are actually quite potent inhibitors. Isoflavones, for example, have demonstrated significant inhibition of tyrosinase monophenolase and diphenolase activities [40].

Collagen and elastin are key elements of the animal extracellular matrix. They are mainly responsible for skin elasticity and resistance [3], and their degradation is one of the main causes of intrinsic skin aging. Their degradation is mainly caused by collagenase and elastase, two enzymes capable of breaking the peptide bonds of collagen and elastin [41]. Table 1 regroups the results of the collagenase and elastase inhibition assays of the argan press-cake and pulp extracts.

The highest collagenase inhibition values were observed with UAE argan press-cake aqueous and methanolic extracts with respective values of (60.97  $\pm$  2.36)% and (52.29  $\pm$  1.71)%, followed by the UAE argan roasted and unroasted press-cake extracts with (31.43  $\pm$  3.06)% and (28.34  $\pm$  2.62)%, respectively. The remaining samples exhibited inhibition values lower than 25%.

As with the tyrosinase inhibition activity mentioned above, this collagenase inhibition activity is probably due to polyphenols in the fruit pulp. These compounds proved to be very good collagenase inhibitors. Indeed, long exposure to harmful stimuli, such as ultraviolet (UV) radiation, activates the overexpression of collagenase and triggers a chain reaction that leads to the degradation of the extracellular matrix, causing skin aging [42]. Polyphenols play a dual role at intra- and extracellular levels by protecting cells from damage caused by UV radiation, while inhibiting the degenerative activity of collagenase.

Elastase belongs to the proteinase family. It is mainly responsible for elastin degradation, and its activity increases with age. This activity results in a decrease in the elasticity of the skin, which causes the appearance of wrinkles [43]. Table 1 tabulates the elastase inhibition percentages of the SFE and UAE argan press-cake and pulp extracts.

The argan press-cake and pulp extracts showed inhibition values below 50%. The UAE aqueous and methanolic pulp extracts demonstrated the highest inhibition values of  $(38.41 \pm 2.18)\%$  and  $(25.02 \pm 1.69)\%$ , respectively, followed by the UAE aqueous, methanolic, and dichloromethanolic extracts, with values ranging between 20 and 3% observed; meanwhile, the SFE extracts showed inhibition values below 1.5%.

These results are similar to those obtained for the tyrosinase and collagenase inhibition assays. These elastase inhibition activities are mainly due to the presence of polyphenols and flavonoids in the argan extracts. Furthermore, the tyrosinase, collagenase and elastase inhibitory activity of these compounds can vary depending on several parameters, including the structural variability of the molecules, their concentrations in the samples, and the presence of several other molecules that can have a synergistic activity.

Moreover, Ghimeray et al. (2015) [44] investigated the anti-collagenase and anti-elastase activities of polyphenols extracted from *Punica granatum*, *Ginkgo biloba*, *Ficus carica*, and *Morus alba*, as well as their combinations. The obtained results by those authors suggested that the combination of different extracts gives rise to higher collagenase inhibition. A concentration of 5  $\mu\text{g}/\text{mL}$  of a mixture of different extracts showed enzymatic inhibitions greater than 65%, probably due to changes in the spatial conformation of collagenase induced by the synergistic effect of polyphenols [45].

The tyrosinase, collagenase, and elastase inhibitory activities of the polyphenols and flavonoids from the argan tree have not yet been cited in the literature. Currently, many cosmetic companies are interested on using elastase, collagenase, and melanogenesis inhibitors as active agents in anti-wrinkle, anti-aging, and skin-lightening products [46]. An increased demand for natural substances having these properties has given rise to several pharmacological investigations, including the current study.

### 3.3. Determination of the Total Phenolic Content

Due to their biological importance in dermocosmetic activities, we chose to orientate our investigation to the polyphenols of argan press-cake and pulp methanolic and aqueous extracts. The results of the polyphenol content evaluation of argan by-products extracts are presented in Table 2.

**Table 2.** Content of total phenolic compounds (TPC) (mean values  $\pm$  standard deviation) expressed in mg gallic acid equivalent per gram of dry matter ( $\text{mg}_{\text{eqAG}}/\text{g}_{\text{DM}}$ ) in argan press cake and fruit pulp.

Sample	TPC ( $\text{mg}_{\text{eqAG}}/\text{g}_{\text{DM}}$ )
UAE Methanol—Unroasted press cake	$7.9 \pm 0.7$
UAE Methanol—Roasted press cake	$3.1 \pm 0.3$
UAE Methanol—Fruit pulp	$68.2 \pm 1.5$
UAE water—Unroasted press cake	$6.5 \pm 0.9$
UAE water—Roasted press cake	$10.3 \pm 1.2$
UAE water—Fruit pulp	$56.8 \pm 3.7$

The argan-fruit pulp extracts showed superior polyphenol contents, with values higher than  $55 \text{ mg}_{\text{eqAG}}/\text{g}_{\text{DM}}$ , whereas press-cake extracts exhibited values ranging between 3 and  $10 \text{ mg}_{\text{eqAG}}/\text{g}_{\text{DM}}$ . These results revealed that the argan pulp extracts have higher amounts of polyphenols, and confirmed the dermocosmetic activities (anti-tyrosinase, anti-collagenase, and anti-elastase) previously described.

These results are consistent with those cited in the literature. A manuscript published by El Monfalouti et al. (2012) [27] featured the total phenolic contents of argan press-cake and pulp extracts. The authors stated that the pulp extract had higher quantity of polyphenols, with a value of  $(75.8 \pm 0.8) \text{ mg}_{\text{eqAG}}/\text{g}_{\text{DM}}$ , whereas the press-cake extract showed a value lower than  $4.8 \pm 0.2 \text{ mg}_{\text{eqAG}}/\text{g}_{\text{DM}}$ .

Additionally, some authors identified the polyphenols of argan pulp and press cake. Charrouf et al. (2007) [47] investigated the chemical composition of the hydroalcoholic extract of argan pulp. They mentioned the presence of protocatechuic acid (21.8%), hyper-

oside (13.4%), isoquercetin (10%), and gallic acid (5%) as lead compounds. Conversely, Rojas et al. (2005) [48] studied the chemical composition of the press-cake hydroalcoholic extract, and found out the presence of the epicatechin (54.72%), vanillic acid (8.10%), p-hydroxybenzoic acid (7.01%), and 4-hydroxybenzyl alcohol (4.27%). Accordingly, these compounds were selected here for molecular docking in order to study their affinities with the enzymes and mechanisms of action.

### 3.4. Molecular Docking Analysis

The molecular docking approach is frequently used in drug design and pharmacogenosy [49]. This approach can be very useful to study the interaction between a ligand and a protein. Molecular docking can be used as an approach for the orientation of biological activities after chemical evaluation and identification of major compounds, or as a tool for studying the mechanisms of action of a molecule after purification and in vitro tests [50]. In the current research effort, molecular docking was used to study the mechanisms of action of compounds previously identified in the argan press-cake and pulp extracts.

For every simulation, a single ligand is docked separately with the protein, then the generated scores and poses are compared with the aim to select the best pose, knowing that the lowest score corresponds to the best binding affinity. Tables 3–5 regroup together the results of such simulations.

**Table 3.** Docking score and binding sites of the different ligands with tyrosinase.

Ligand	Score (Kcal/mol)	Active Site Residues Involved in H-Bond
Epicatechin	−6.7	His259, His263, Arg268, Met280
Vanillic acid	−5.8	ND
p-hydroxybenzoic acid	−6.0	ND
4-hydroxybenzyl alcohol	−5.6	His61, His85
Hyperoside	−6.3	His85, His263, Met280
Isoquercetin	−6.3	Met280, Gly281, Val283
Protocatechic acid	−3.3	His85, His259, Asn260, Phe264, His263
Gallic acid	−5.9	His85, Phe264

**Table 4.** Docking score and binding sites of the different ligands with collagenase.

Ligand	Score (Kcal/mol)	Active Site Residues Involved in H-Bond
Epicatechin	−8.5	Asn180, Ala182, His218, Tyr237, Tyr240
Vanillic acid	−6.5	Val101, Leu226, His228
p-hydroxybenzoic acid	−6.7	Leu181, Ala182, Arg214, His218, Glu219, Ser239
4-hydroxybenzyl alcohol	−6.2	His218
Hyperoside	−9.2	Ala182, Ala184, His222, His228
Isoquercetin	−10.5	Asn180, His183, Asp186, His228, Pro238
Protocatechic acid	−6.4	Leu181, Ala182, Arg214, Val215
Gallic acid	−7.1	Leu181, Ala182, Arg214, Glu219

**Table 5.** Docking score and binding sites of the different ligands with elastase.

Ligand	Score (Kcal/mol)	Active Site Residues Involved in H-Bond
Epicatechin	−6.5	Ser190, Asn192, Ser195, Cys220
Vanillic acid	−5.2	Asn192, Ser195
p-hydroxybenzoic acid	−4.8	Cys220
4-hydroxybenzyl alcohol	−4.9	His57, Ser190, Ser195, Ser214
Hyperoside	−7.7	His57, Ser190, Asn192, Ser195, Ser214, Gly219
Isoquercetin	−7.8	Arg143, Asn147, Cys191, Ser195, Cys220
Protocatechic acid	−5.3	Asn192, Cys216
Gallic acid	−5.7	Asn192, Ser195

The results of the tyrosinase bindings showed that the ligand with the best affinity was the epicatechin with an affinity score of  $-6.7$  Kcal/mol (Figure 5), followed by the hyperoside, isoquercetin, and protocatechuic acid with a value of  $-6.3$  Kcal/mol. The visualization of the amino acids involved on the ligand–protein interaction showed that some amino acids are common to some compounds. For example, epicatechin and hyperoside both bind with His263 and Met280. Conversely, His259 and His263 are common to epicatechin and protocatechuic acid. These results revealed that those compounds have similarities on their binding sites, which may suggest that they may have similar inhibition mechanisms of action.

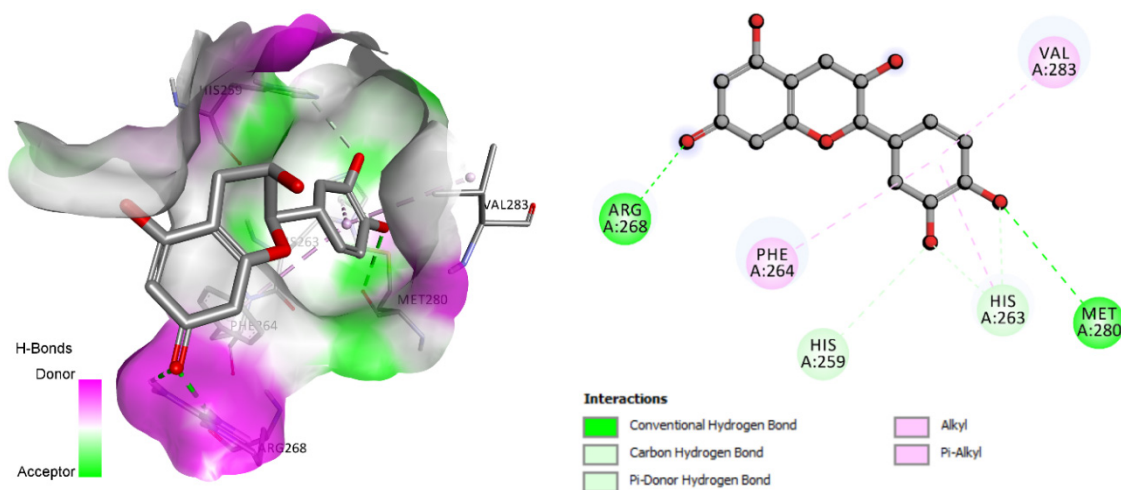


**Figure 5.** 3D and 2D protein–ligand interactions at the tyrosinase active site of the epicatechin (PDB CID: 2Y9X).

Kojic acid is an inhibitor of tyrosinase. It is widely used as positive control for tyrosinase inhibition assays, and its mechanism of action has been reported in the literature by Ashooriha et al. (2020) [51]. According to these authors, this compound has an affinity score of  $-4.09$  kcal/mol, and binds with the amino acids His85, His259, His263, and Met280. These amino acids are common to our ligands, which suggest that they all may have the same inhibition mechanism of action.

The affinity scores analysis of the ligands after docking simulations with collagenase showed the lowest value compared to other ligands—isoquercetin with  $-10.5$  Kcal/mol (Figure 6), followed by hyperoside with  $-9.2$  Kcal/mol. The obtained results confirm the strong affinity of isoquercetin and hyperoside with the collagenase enzyme by the common amino acid His228. Other ligands showed scores superior to  $-8.0$  Kcal/mol, with a value of  $-8.5$  Kcal/mol for the epicatechin.

According to the literature, polyphenols and flavonoids have a high affinity with collagenase. Furthermore, several in vitro evaluations have shown that these metabolites have collagenase inhibitory activity [52–54]. Along to the same line of research, molecular docking tests on different flavonoids were achieved by Priani and Fakhri (2021) [55]. They reported docking scores ranging between  $-8$  and  $-10$  Kcal/mol. In another study published by Taherkhani et al. (2020) [56], isoquercetin and epicatechin showed respective scores of  $-8.96$  and  $-6.4$  Kcal/mol. These data are in perfect agreement with the results here obtained for isoquercetin and epicatechin.

Comparison of different data obtained after docking simulations of the ligands with elastase disclosed that the lowest affinity score was obtained with isoquercetin ( $-7.8$  Kcal/mol) (Figure 7), followed by hyperoside and epicatechin with  $-7.7$  and  $-6.5$  Kcal/mol, respectively. Moreover, these ligands are bonded with elastase, using more than 4 covalent bonds, with a common amino acid, Ser195.

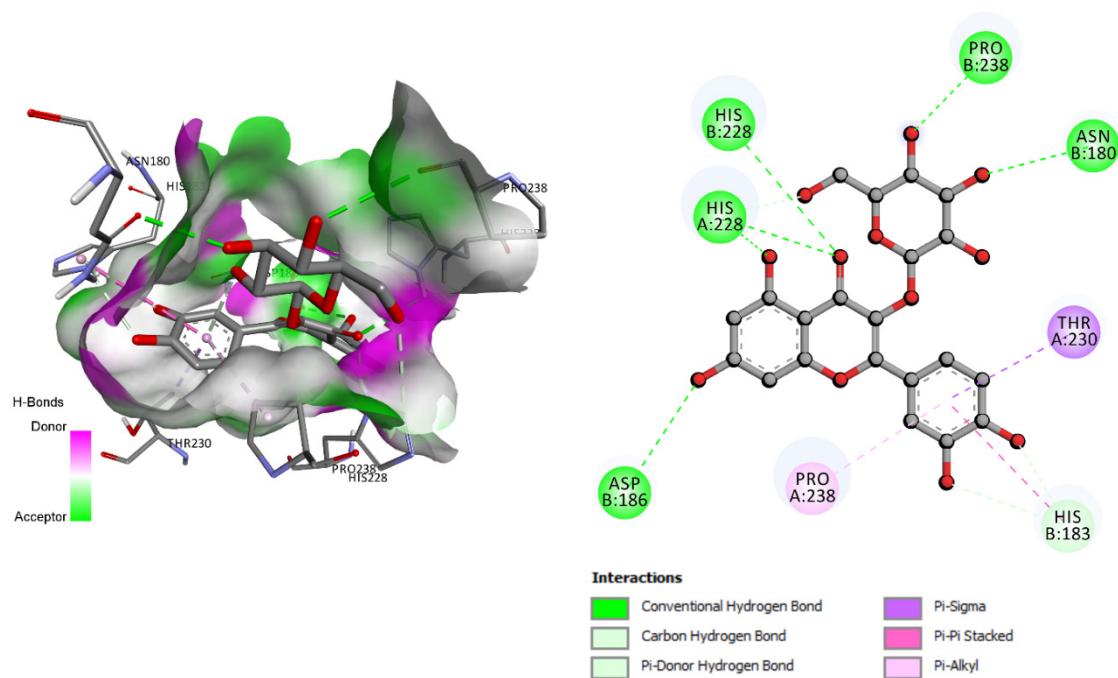


**Figure 6.** 3D and 2D protein–ligand interactions at the collagenase active site of the isoquercetin (PDB CID: 1CGL).

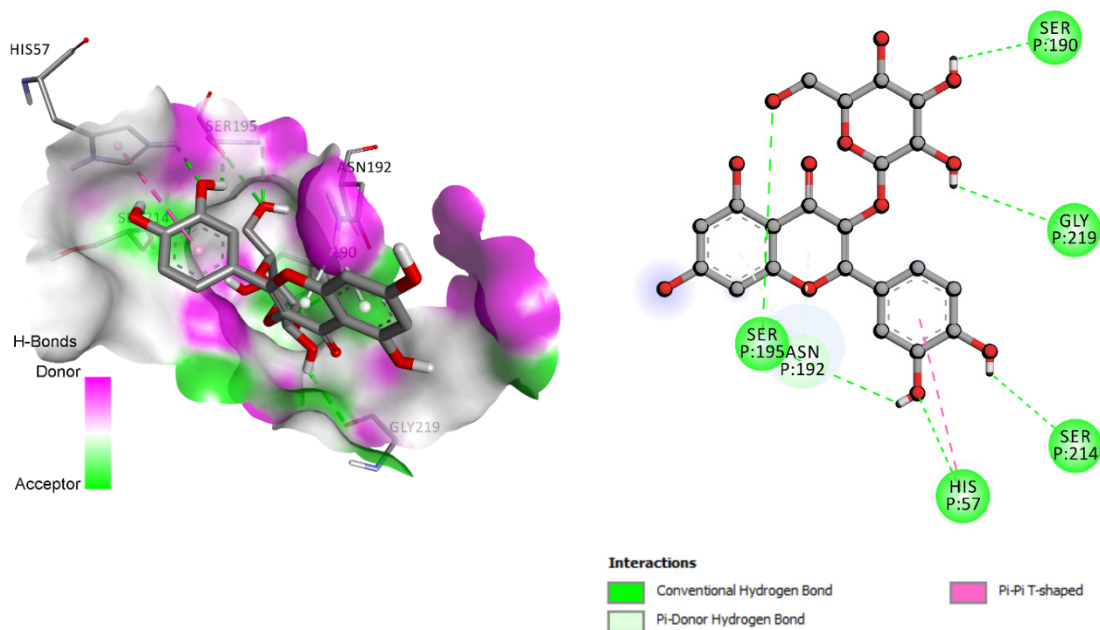


**Figure 7.** 3D and 2D protein–ligand interactions at the elastase active site of the hyperoside (PDB CID: 1BRU).

Molecular docking simulations of flavonoids and polyphenols with elastase have also been reported in the literature. Elastase and collagenase are the main causes of intrinsic aging. Evaluations by molecular docking aimed to identify molecules that can interact with the active sites of these enzymes to inhibit them [57]. According to a study reported by Priani and Fakih (2021) [55], glycosylated flavonoids showed docking score values between  $-5.5$  and  $-6.5$  Kcal/mol. In another study conveyed by Bras et al. (2010) [58] different molecules of procyanidins (condensed tannins containing a molecule of catechol) were evaluated for their affinities with elastase. The obtained results showed values between  $-3$  and  $-5$  Kcal/mol. Moreover, molecules with high molecular weight showed the most

interesting scores. Such a finding may probably be due to the strong binding caused by the establishment of contact points with the amino acids present in their active sites.

#### 4. Conclusions

In conclusion, the supercritical fluid and ultrasound-assisted methods afford extracts with good yields, especially the ultrasound-assisted extraction. The supercritical fluid extraction was used since it is the most environmentally friendly and allowed us to recover compounds from argan press cake; however, the extract showed very low enzyme inhibition activity. In contrast, the argan pulp extracts obtained with ultrasound-assisted extraction disclosed promising results. Indeed, the argan pulp methanolic and aqueous extracts revealed very interesting tyrosinase, collagenase, and elastase inhibition activities at 200 µg/mL with values higher than 20 times those observed with press-cake extracts. Additionally, the evaluation of the phenolic contents confirmed their presence in the pulp extracts in high amounts. The polyphenols have been widely cited by researchers for their tyrosinase, collagenase, and elastase inhibition potentials.

A molecular docking study was performed, aiming to predict the mechanism of action behind the argan by-product extracts' inhibition activity. The obtained results showed that hyperoside and isoquercetin (lead compounds of the argan-fruit pulp) have the highest affinity with tyrosinase, collagenase, and elastase in comparison with the other tested compounds. These results correlate positively with the inhibition percentages observed after the *in vitro* tests. This manuscript highlights the potential of argan by-products using a combined computational/biological approach. Despite showing moderate activities, the exploitation of argan press cake and pulp as natural ingredients for cosmetics could be an added value to their traditional uses which can be incorporated into Moroccan practices for a sustainable economic system in a context where argan-based products are highly demanded in the market.

**Author Contributions:** Conceptualization, N.E.A. and H.M.; methodology, N.E.A.; software, H.M.; validation, M.E.Y. and A.E.H.; formal analysis, J.M.R.; investigation, N.E.A., H.M. and S.H.; resources, N.E.A.; data curation, J.M.R.; writing—original draft preparation, H.M.; writing—review and editing, N.E.A., J.R.G.d.S.A. and J.M.R.; visualization, H.M. and S.H.; supervision, N.E.A.; project administration, N.E.A.; funding acquisition, N.E.A. and J.M.R. All authors have read and agreed to the published version of the manuscript.

**Funding:** This research was partially funded by EXANDAS-H2020-MSCA-RISE-2015—“Exploitation of aromatic plants' by-products for the development of novel cosmeceuticals and food supplements” (Grant Agreement No 691247). This work is also based upon the work from COST Action 18101 SOURDOMICS—Sourdough biotechnology network towards novel, healthier and sustainable food and bioprocesses (<https://sourdomics.com/>; <https://www.cost.eu/actions/CA18101/>, where the author J.M.R. is the Chair and Grant Holder Scientific Representative, and the author N.E.A. is member of the Working Groups 3, 4 and 7, and is supported by COST (European Cooperation in Science and Technology) (<https://www.cost.eu/>). COST is a funding agency for research and innovation networks.

**Institutional Review Board Statement:** Not applicable.

**Informed Consent Statement:** Not applicable.

**Data Availability Statement:** Data is contained within the article.

**Conflicts of Interest:** The authors declare no conflict of interest.

#### References

1. Venus, M.; Waterman, J.; McNab, I. Basic physiology of the skin. *Surgery (Oxford)* **2010**, *28*, 469–472. [[CrossRef](#)]
2. Escoffier, C.; de Rigal, J.; Rochefort, A.; Vasselet, R.; Lévêque, J.-L.; Agache, P.G. Age-related mechanical properties of human skin: An *in vivo* study. *J. Invest. Dermatol.* **1989**, *93*, 353–357. [[CrossRef](#)]
3. Farage, M.A.; Miller, K.W.; Elsner, P.; Maibach, H.I. Structural Characteristics of the Aging Skin: A Review. *Cutan. Ocul. Toxicol.* **2007**, *26*, 343–357. [[CrossRef](#)] [[PubMed](#)]

4. Buffoli, B.; Rinaldi, F.; Labanca, M.; Sorbellini, E.; Trink, A.; Guanziroli, E.; Rezzani, R.; Rodella, L.F. The human hair: From anatomy to physiology. *Int. J. Dermatol.* **2013**, *53*, 331–341. [[CrossRef](#)] [[PubMed](#)]
5. Ebling, F.J.G. The Biology of Hair. *Dermatol. Clin.* **1987**, *5*, 467–481. [[CrossRef](#)]
6. Sjerobabski-Masneć, I.; Šitum, M. Skin aging. *Acta Clin. Croat.* **2010**, *49*, 515–518. [[PubMed](#)]
7. Tobin, D.J. Introduction to skin aging. *J. Tissue Viability* **2017**, *26*, 37–46. [[CrossRef](#)]
8. Tobin, D.J. Biochemistry of human skin—Our brain on the outside. *Chem. Soc. Rev.* **2006**, *35*, 52–67. [[CrossRef](#)]
9. Boucetta, K.Q.; Charrouf, Z.; Derouiche, A.; Rahali, Y.; Bensouda, Y. Skin hydration in postmenopausal women: Argan oil benefit with oral and/or topical use. *Menopausal Rev.* **2014**, *5*, 280–288. [[CrossRef](#)]
10. El Hafian, M.; Benlandini, N.; Elyacoubi, H.; Zidane, L.; Rochdi, A. Étude floristique et ethnobotanique des plantes médicinales utilisées au niveau de la préfecture d’Agadir-Ida-Outanane (Maroc). *J. Appl. Biosci.* **2014**, *81*, 7198. [[CrossRef](#)]
11. Moukal, A. L’arganier, *Argania spinosa* L. (skeels), usage thérapeutique, cosmétique et alimentaire. *Phytothérapie* **2004**, *2*, 135–141. [[CrossRef](#)]
12. Ouhaddou, H.; Boubaker, H.; Msanda, F.; El Mousadik, A. An ethnobotanical study of medicinal plants of the Agadir Ida Ou Tanane province (southwest Morocco). *J. Appl. Biosci.* **2015**, *84*, 7707. [[CrossRef](#)]
13. Silva, A.R.; Grosso, C.; Delerue-Matos, C.; Rocha, J.M. Comprehensive review on the interaction between natural compounds and brain receptors: Benefits and toxicity. *Eur. J. Med. Chem.* **2019**, *174*, 87–115. [[CrossRef](#)] [[PubMed](#)]
14. Masuda, T.; Odaka, Y.; Ogawa, N.; Nakamoto, K.; Kuninaga, H. Identification of Geranic Acid, a Tyrosinase Inhibitor in Lemongrass (*Cymbopogon citratus*). *J. Agric. Food Chem.* **2007**, *56*, 597–601. [[CrossRef](#)] [[PubMed](#)]
15. Michailidis, D.; Angelis, A.; Aligiannis, N.; Mitakou, S.; Skaltsounis, L. Recovery of Sesamin, Sesamol, and Minor Lignans From Sesame Oil Using Solid Support-Free Liquid–Liquid Extraction and Chromatography Techniques and Evaluation of Their Enzymatic Inhibition Properties. *Front. Pharmacol.* **2019**, *10*, 723. [[CrossRef](#)] [[PubMed](#)]
16. Gendron, R.; Grenier, D.; Sorsa, T.; Mayrand, D. Inhibition of the Activities of Matrix Metalloproteinases 2, 8, and 9 by Chlorhexidine. *Clin. Diagn. Lab. Immunol.* **1999**, *6*, 437–439. [[CrossRef](#)] [[PubMed](#)]
17. Angelis, A.; Hubert, J.; Aligiannis, N.; Michalea, R.; Abedini, A.; Nuzillard, J.-M.; Gangloff, S.C.; Skaltsounis, A.-L.; Renault, J.-H. Bio-Guided Isolation of Methanol-Soluble Metabolites of Common Spruce (*Picea abies*) Bark by-Products and Investigation of Their Dermo-Cosmetic Properties. *Molecules* **2016**, *21*, 1586. [[CrossRef](#)]
18. Vermerris, W.; Nicholson, R. *Biosynthesis of Phenolic Compounds*; Springer Science and Business Media LLC: Dordrecht, The Netherlands, 2008; pp. 63–149.
19. Trott, O.; Olson, A.J. AutoDock Vina: Improving the speed and accuracy of docking with a new scoring function, efficient optimization, and multithreading. *J. Comput. Chem.* **2010**, *31*, 455–461. [[CrossRef](#)]
20. Yu, Q.; Fan, L.; Duan, Z. Five individual polyphenols as tyrosinase inhibitors: Inhibitory activity, synergistic effect, action mechanism, and molecular docking. *Food Chem.* **2019**, *297*, 124910. [[CrossRef](#)]
21. Osorio, E.; Bravo, K.; Cardona, W.; Yepes, A.; Coa, J.C. Antiaging activity, molecular docking, and prediction of percutaneous absorption parameters of quinoline–hydrazone hybrids. *Med. Chem. Res.* **2019**, *28*, 1959–1973. [[CrossRef](#)]
22. Karatoprak, G.Ş.; Göger, F.; Çelik, I.; Budak, Ü.; Akkol, E.K.; Aschner, M. Phytochemical profile, antioxidant, antiproliferative, and enzyme inhibition-docking analyses of *Salvia ekimiana* Celep & Doğan. *S. Afr. J. Bot.* **2021**, *146*, 36–47. [[CrossRef](#)]
23. Gharby, S.; Harhar, H.; Guillaume, D.; Haddad, A.; Charrouf, Z. The Origin of Virgin Argan Oil’s High Oxidative Stability Unraveled. *Nat. Prod. Commun.* **2012**, *7*, 621–624. [[CrossRef](#)] [[PubMed](#)]
24. Taribak, C.; Casas, L.; Mantell, C.; Elfadli, Z.; Metni, R.E.; de la Ossa, E.M. Quality of Cosmetic Argan Oil Extracted by Supercritical Fluid Extraction from *Argania spinosa* L. *J. Chem.* **2013**, *2013*, 408194. [[CrossRef](#)]
25. Harhar, H.; Gharby, S.; Ghanmi, M.; EL Monfalouti, H.; Guillaume, D.; Charrouf, Z. Composition of the Essential Oil of *Argania spinosa* (Sapotaceae) Fruit Pulp. *Nat. Prod. Commun.* **2010**, *5*, 935–936. [[CrossRef](#)] [[PubMed](#)]
26. Harhar, H.; Gharby, S.; Kartah, B.; El Monfalouti, H.; Guillaume, D.; Charrouf, Z. Influence of Argan Kernel Roasting-time on Virgin Argan Oil Composition and Oxidative Stability. *Mater. Veg.* **2011**, *66*, 163–168. [[CrossRef](#)]
27. El Monfalouti, H.; Charrouf, Z.; Belviso, S.; Ghirardello, D.; Scursatone, B.; Guillaume, D.; Denhez, C.; Zeppa, G. Analysis and antioxidant capacity of the phenolic compounds from argan fruit (*Argania spinosa* (L.) Skeels). *Eur. J. Lipid Sci. Technol.* **2012**, *114*, 446–452. [[CrossRef](#)]
28. Ito, S.; Wakamatsu, K. Quantitative Analysis of Eumelanin and Pheomelanin in Humans, Mice, and Other Animals: A Comparative Review. *Pigment Cell Res.* **2003**, *16*, 523–531. [[CrossRef](#)]
29. Gillbro, J.M.; Olsson, M.J. The melanogenesis and mechanisms of skin-lightening agents—Existing and new approaches. *Int. J. Cosmet. Sci.* **2011**, *33*, 210–221. [[CrossRef](#)]
30. Hearing, V.J.; Jiménez, M. Mammalian tyrosinase—The critical regulatory control point in melanocyte pigmentation. *Int. J. Biochem.* **1987**, *19*, 1141–1147. [[CrossRef](#)]
31. Bourhim, T.; Villareal, M.O.; Gadhi, C.; Hafidi, A.; Isoda, H. Depigmenting effect of argan press-cake extract through the down-regulation of Mitf and melanogenic enzymes expression in B16 murine melanoma cells. *Cytotechnology* **2018**, *70*, 1389–1397. [[CrossRef](#)]
32. Di Petrillo, A.; González-Paramás, A.M.; Era, B.; Medda, R.; Pintus, F.; Santos-Buelga, C.; Fais, A. Tyrosinase inhibition and antioxidant properties of *Asphodelus microcarpus* extracts. *BMC Complement. Altern. Med.* **2016**, *16*, 453. [[CrossRef](#)] [[PubMed](#)]

33. Wang, Y.; Curtis-Long, M.J.; Lee, B.W.; Yuk, H.J.; Kim, D.W.; Tan, X.F.; Park, K.H. Inhibition of tyrosinase activity by polyphenol compounds from *Flemingia philippinensis* roots. *Bioorg. Med. Chem.* **2014**, *22*, 1115–1120. [[CrossRef](#)] [[PubMed](#)]
34. Tang, H.; Cui, F.; Li, H.; Huang, Q.; Li, Y. Understanding the inhibitory mechanism of tea polyphenols against tyrosinase using fluorescence spectroscopy, cyclic voltammetry, oximetry, and molecular simulations. *RSC Adv.* **2018**, *8*, 8310–8318. [[CrossRef](#)]
35. Madani, W.; Kermasha, S.; Bisakowski, B. Inhibition of tyrosinase activity by a polyphenol esterase using selected phenolic substrates. *Phytochemistry* **1999**, *52*, 1001–1008. [[CrossRef](#)]
36. Jeong, C.H.; Shim, K.H. Tyrosinase Inhibitor Isolated from the Leaves of *Zanthoxylum piperitum*. *Biosci. Biotechnol. Biochem.* **2004**, *68*, 1984–1987. [[CrossRef](#)]
37. Chang, T.-S. An Updated Review of Tyrosinase Inhibitors. *Int. J. Mol. Sci.* **2009**, *10*, 2440–2475. [[CrossRef](#)]
38. Seo, S.-Y.; Sharma, V.K.; Sharma, N. Mushroom Tyrosinase: Recent Prospects. *J. Agric. Food Chem.* **2003**, *51*, 2837–2853. [[CrossRef](#)]
39. Şöhretoğlu, D.; Sari, S.; Barut, B.; Özel, A. Tyrosinase inhibition by some flavonoids: Inhibitory activity, mechanism by in vitro and in silico studies. *Bioorg. Chem.* **2018**, *81*, 168–174. [[CrossRef](#)]
40. Chang, T.-S.; Ding, H.-Y.; Tai, S.S.-K.; Wu, C.-Y. Mushroom tyrosinase inhibitory effects of isoflavones isolated from soygerm koji fermented with *Aspergillus oryzae*. *BCRC Food Chem.* **2007**, *105*, 1430–1438. [[CrossRef](#)]
41. Tortora, G.J.; Funke, B.R.; Case, C.L. *Microbiology: An Introduction*; Pearson Benjamin Cummings: San Francisco, CA, USA, 2007.
42. Imokawa, G.; Ishida, K. Biological Mechanisms Underlying the Ultraviolet Radiation-Induced Formation of Skin Wrinkling and Sagging I: Reduced Skin Elasticity, Highly Associated with Enhanced Dermal Elastase Activity, Triggers Wrinkling and Sagging. *Int. J. Mol. Sci.* **2015**, *16*, 7753–7775. [[CrossRef](#)]
43. Xu, G.-H.; Kim, Y.-H.; Choo, S.-J.; Ryoo, I.-J.; Yoo, J.-K.; Ahn, J.-S.; Yoo, I.-D. Chemical constituents from the leaves of *Ilex paraguariensis* inhibit human neutrophil elastase. *Arch. Pharmacol. Res.* **2009**, *32*, 1215–1220. [[CrossRef](#)] [[PubMed](#)]
44. Ghimeray, A.K.; Jung, U.S.; Lee, H.Y.; Kim, Y.H.; Ryu, E.K.; Chang, M.S. In vitro antioxidant, collagenase inhibition, and in vivo anti-wrinkle effects of combined formulation containing *Punica granatum*, *Ginkgo biloba*, *Ficus carica*, and *Morus alba* fruits extract. *Clin. Cosmet. Investig. Dermatol.* **2015**, *8*, 389–396. [[CrossRef](#)] [[PubMed](#)]
45. Madhan, B.; Krishnamoorthy, G.; Rao, J.R.; Nair, B.U. Role of green tea polyphenols in the inhibition of collagenolytic activity by collagenase. *Int. J. Biol. Macromol.* **2007**, *41*, 16–22. [[CrossRef](#)] [[PubMed](#)]
46. Michalak, M.; Pierzak, M.; Kręcis, B.; Suliga, E. Bioactive Compounds for Skin Health: A Review. *Nutrients* **2021**, *13*, 203. [[CrossRef](#)]
47. Charrouf, Z.; Hilali, M.; Jauregui, O.; Soufiaoui, M.; Guillaume, D. Separation and characterization of phenolic compounds in argan fruit pulp using liquid chromatography–negative electrospray ionization tandem mass spectroscopy. *Food Chem.* **2007**, *100*, 1398–1401. [[CrossRef](#)]
48. Rojas, L.B.; Quideau, S.; Pardon, A.P.; Charrouf, Z. Colorimetric Evaluation of Phenolic Content and GC-MS Characterization of Phenolic Composition of Alimentary and Cosmetic Argan Oil and Press Cake. *J. Agric. Food Chem.* **2005**, *53*, 9122–9127. [[CrossRef](#)]
49. Ferreira, L.G.; Dos Santos, R.N.; Oliva, G.; Andricopulo, A.D. Molecular Docking and Structure-Based Drug Design Strategies. *Molecules* **2015**, *20*, 13384–13421. [[CrossRef](#)]
50. Yuriev, E.; Holien, J.; Ramslund, P.A. Improvements, trends, and new ideas in molecular docking: 2012–2013 in review. *J. Mol. Recognit.* **2015**, *28*, 581–604. [[CrossRef](#)]
51. Ashooriha, M.; Khoshneviszadeh, M.; Khoshneviszadeh, M.; Rafiei, A.; Kardan, M.; Yazdian-Robati, R.; Emami, S. Kojic acid–natural product conjugates as mushroom tyrosinase inhibitors. *Eur. J. Med. Chem.* **2020**, *201*, 112480. [[CrossRef](#)]
52. Sin, B.Y.; Kim, H.P. Inhibition of collagenase by naturally-occurring flavonoids. *Arch. Pharmacol. Res.* **2005**, *28*, 1152–1155. [[CrossRef](#)]
53. Lim, H.; Kim, H.P. Inhibition of Mammalian Collagenase, Matrix Metalloproteinase-1, by Naturally-Occurring Flavonoids. *Planta Med.* **2007**, *73*, 1267–1274. [[CrossRef](#)] [[PubMed](#)]
54. Nguyen, T.T.H.; Moon, Y.-H.; Ryu, Y.-B.; Kim, Y.-M.; Nam, S.-H.; Kim, M.-S.; Kimura, A.; Kim, D. The influence of flavonoid compounds on the in vitro inhibition study of a human fibroblast collagenase catalytic domain expressed in *E. coli*. *Enzym. Microb. Technol.* **2013**, *52*, 26–31. [[CrossRef](#)] [[PubMed](#)]
55. Priani, S.E.; Fakhri, T.M. Insights into Molecular Interaction of Flavonoid Compounds in Citrus Peel Bound to Collagenase and Elastase Enzymes: A Computational Study. *Pharm. Sci. Res.* **2021**, *8*, 5.
56. Taherkhani, A.; Moradkhani, S.; Orangi, A.; Jalalvand, A.; Khamverdi, Z. Molecular docking study of flavonoid compounds for possible matrix metalloproteinase-13 inhibition. *J. Basic Clin. Physiol. Pharmacol.* **2020**, *32*, 1105–1119. [[CrossRef](#)] [[PubMed](#)]
57. Tundis, R.; Loizzo, M.R.; Bonesi, M.; Menichini, F. Potential Role of Natural Compounds Against Skin Aging. *Curr. Med. Chem.* **2015**, *22*, 1515–1538. [[CrossRef](#)] [[PubMed](#)]
58. Bras, N.F.; Goncalves, R.; Mateus, N.; Fernandes, P.A.; Ramos, M.J.; de Freitas, V. Inhibition of pancreatic elastase by polyphenolic compounds. *J. Agric. Food Chem.* **2010**, *58*, 10668–10676. [[CrossRef](#)]